Fluid Modelling of Dielectric Barrier Discharges for Plasma Technology

A. P. Jovanović*, M. N. Stankov, D. Loffhagen, M. M. Becker
Leibniz Institute for Plasma Science and Technology (INP), Greifswald, Germany

*Corresponding author: aleksandar.jovanovic@inp-greifswald.de

Abstract

COMSOL Multiphysics® with LiveLink™ for MATLAB® is used for the numerical analysis of dielectric barrier discharges (DBDs). The applied fluid-Poisson model comprises balance equations for the particle number densities of relevant plasma species, the electron energy density, and the density of surface charges accumulating at the dielectric surfaces. The set of balance equations is coupled with Poisson's equation for a self-consistent determination of the electric field. Physics-based boundary conditions and initial values are applied to close the coupled system of partial differential equations. The application of COMSOL Multiphysics® for studying large system with tens of species and hundreds of reactions is simplified by the in-house toolbox MCPlas, which combines the features of MATLAB® and COMSOL Multiphysics® via LiveLink™ for MATLAB®. The present contribution highlights how MCPlas is used to build up time-dependent DBD models in spatially one-dimensional (1D) and axisymmetric two-dimensional (2D) geometry. The COMSOL models thus generated are used to study diffuse and filamentary DBDs in argon at different conditions.

Introduction

Dielectric barrier discharges (DBDs) are frequently used to generate non-thermal plasmas for technological applications, such as ozone generation, surface processing and plasma medicine [1–3]. DBDs are characterized by the presence of a dielectric layer on at least one electrode, which limits the electric current and prevents arcing. Depending on the conditions, DBDs can be diffuse or filamentary. Due to their broad use, it is of crucial importance to get a detailed understanding of the physical and chemical processes occurring in DBDs. One of the ways to do this is by using fluid modelling [4–7]. The computational efficiency of fluid models allows one to take into account complex physical and chemical processes occurring during the plasma production, which makes them suitable for practical applications. Here, fluid models are used for the modelling of DBDs at different conditions using equation-based modelling in COMSOL Multiphysics®.

Depending on the complexity of the model, which can take into account a large number of particle species (tens to hundreds) and processes (hundreds to thousands), the definition of the equations becomes a tedious and error-prone process. To overcome this problem, the MCPlas toolbox is developed. MCPlas consists of a number of MATLAB scripts using the functionality provided by the LiveLink™ for MATLAB® module. In order to illustrate the use of this code, two examples are presented, 1) a diffuse DBD in argon and 2) a filamentary atmospheric-pressure DBD in argon. The paper is structured as follows. First, the fluid-Poisson model is described showing the governing equations, boundary and initial conditions. The following section introduces the MCPlas toolbox by illustrating the structure of the code and describing its main features. In the next section, two case studies are carried out and the results are presented. Finally, main conclusions are given.

Model equations and numerical procedure

A fluid model coupled with Poisson's equation is applied in order to describe the plasma-physical processes occurring in DBDs [7]. The system of equations consists of continuity equations for the particles number densities n_p of relevant plasma species

$$\frac{\partial n_p}{\partial t} + \nabla \cdot \mathbf{\Gamma}_p = S_p, \tag{1}$$

the electron energy balance equation for the energy density of electrons w_e

$$\frac{\partial w_e}{\partial t} + \nabla \cdot \mathbf{Q}_e = -e_0 \mathbf{E} \cdot \mathbf{\Gamma}_e + \widetilde{S}_e \tag{2}$$

and Poisson's equation for the electric potential ϕ

$$-\varepsilon_0 \varepsilon_r \nabla^2 \phi = \sum_p q_p n_p. \tag{3}$$

Here, $\mathbf{\Gamma}_p$ and $\mathbf{Q}_e$ are the particle fluxes and the electron energy flux, S_p and $\widetilde{S}_e$ are source terms describing the gain and loss of particles and electron energy in reaction kinetic processes, e_0 denotes the elementary charge, $\mathbf{E} = -\nabla\phi$ is the electric field, ε_0 and ε_r represent the vacuum permittivity and relative permittivity of the medium, respectively, and q_p is the charge of particle species p. For the fluxes of particles and the energy flux, the drift-diffusion approximation

$$\mathbf{\Gamma}_p = \mathrm{sgn}(q_p)\, b_p \mathbf{E}\, n_p - \nabla(D_p\, n_p) \tag{4}$$

$$\mathbf{Q}_e = -\widetilde{b}_e \mathbf{E}\, n_e - \nabla(\widetilde{D}_e\, n_e), \tag{5}$$

is used, where b_p and D_p are the mobility and diffusion coefficients for particle species p, and $\widetilde{b}_e$ and $\widetilde{D}_e$ are the mobility and diffusion coefficient for energy transport of electrons, respectively. In addition to these equations, the balance equation for surface charges with density σ accumulating on the dielectric surfaces is solved at the plasma-dielectric interface

$$\frac{\partial \sigma}{\partial t} = \sum_p q_p \mathbf{\Gamma}_p \cdot \boldsymbol{\nu}, \tag{6}$$

where $\boldsymbol{\nu}$ is the outward normal to the boundary surface.

A set of physically motivated boundary conditions and initial values are applied to complete the coupled system of partial differential equations. For Poisson's equation, Dirichlet boundary conditions are set, i.e. the potential is set to $\phi = 0$ at the grounded electrode, and $\phi = U_a(t)$ at the powered electrode. In addition, the flux source boundary condition $-\varepsilon_0\varepsilon_r\mathbf{E}\cdot\boldsymbol{\nu} = \sigma$ is used at the plasma-dielectric interface to account for the change of the electric field due to accumulated charges. For the particle balance equations, boundary conditions according to Hagelaar *et al.* are applied [7, 8]:

1. for heavy particle species

$$\boldsymbol{\nu}\cdot\boldsymbol{\Gamma}_i = \frac{1-r_i}{1+r_i}\left(|\mathrm{sgn}(q_i)b_i\mathbf{E}n_i| + v_{th,i}n_i\right) \tag{7}$$

2. for electrons

$$\boldsymbol{\nu}\cdot\boldsymbol{\Gamma}_e = \frac{1-r_e}{1+r_e}\left(|b_e\mathbf{E}n_e| + v_{th,e}n_e\right) - \frac{2}{1+r_e}\sum_i \max(\gamma_i\boldsymbol{\Gamma}_i\cdot\boldsymbol{\nu}, 0) \tag{8}$$

3. for electron energy balance equation

$$\boldsymbol{\nu}\cdot\mathbf{Q}_e = \frac{1-r_e}{1+r_e}\left(|\widetilde{b}_e\mathbf{E}n_e| + \widetilde{v}_{th,e}n_e\right) - \frac{2}{1+r_e}u_e^{\gamma}\sum_i \max(\gamma_i\boldsymbol{\Gamma}_i\cdot\boldsymbol{\nu}, 0)\,. \tag{9}$$

Here, v_{th} is the thermal velocity of the respective species, $\widetilde{v}_{th,e} = 2k_BT_ev_{th,e}$, T_e is the electron temperature, k_B is the Boltzmann constant, $r_{e,i}$ are the reflection coefficients, γ is the secondary electron emission coefficient, while u_e^{γ} denotes the mean energy of secondary electrons. As initial conditions, quasi-neutral conditions with uniform number density for all particle species are used. Similarly, the energy density is assumed to be uniform.

The complete set of equations is implemented and solved using equation-based modelling in COMSOL. For the spatial discretization, linear Lagrange elements are used for the continuity equations and the electron energy balance equation, quadratic Lagrange elements are applied for Poisson's equation, and discontinuous Lagrange elements of first order are employed for the balance equation for surface charges. For the temporal discretization, the backward differentiation formula method with adaptive order varying between 1 and 5 is applied. The equations are solved in coupled manner. The time-dependent solver utilizes the fully coupled constant Newton method with damping factor equal to 1 and the direct solver PARDISO. The prescribed absolute and relative tolerances are set to 10^{-4}. Note that the balance equations are solved in logarithmic form to achieve better stability.

MCPlas toolbox

The MATLAB-COMSOL toolbox for plasma modelling, MCPlas, is developed in MATLAB and uses the COMSOL module LiveLink™ for MATLAB® to set up the equation-based COMSOL model. The workflow for the implementation of a plasma model in COMSOL using MCPlas is visualized in Figure 1. The first step in the MATLAB code is the reading of the input data, which considers a list of particle species and their properties, plasma-chemical reactions together with rate coefficients and transport coefficients. It is important to note that the implementation of all balance equations with corresponding reaction kinetic processes is automated using the previously prepared species list and reaction scheme. Besides a timesaving aspect, the applied automation excludes the possibility for errors, which are characteristic for manual implementations of complex reaction kinetics. In further steps, different parameters describing the geometry of the problem and properties of the discharge are added. After these steps, the LiveLink™ for MATLAB® module is employed to build up a COMSOL model by setting up the model equations and the definition of all parameters for the numerical solver. Note that MCPlas is able to automatically generate plasma models in COMSOL involving an arbitrary number of species and reaction kinetic processes depending on the general input files defined by the user.

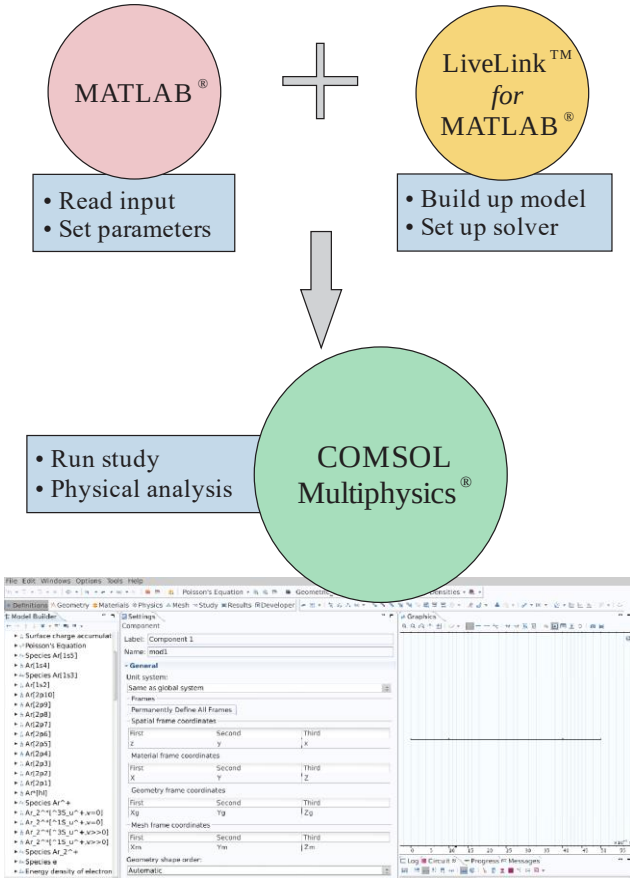

Figure 1.Workflow of plasma modelling using MCPlas.

Results and Discussion

The main goal of this contribution is to present how COMSOL with the LiveLink™ for MATLAB® module and MATLAB are used by MCPlas to automatically generate time-dependent DBD models for the analysis of such discharges often used in plasma-technological applications. Two test cases are considered, which are presented in the following subsections.

Case 1: Modelling of a diffuse DBD in argon at 500 mbar

The first test case for the model generated by MCPlas is the spatially 1D modelling of a DBD in plane-parallel

configuration, where both electrodes are covered by glass dielectrics as illustrated in Figure 2. The gap between the 1 mm thin dielectric layers is 3 mm. The sinusoidal voltage $U_a(t) = U_0 \sin(2\pi ft)$ is applied at the left electrode, while the right one is grounded. The applied voltage has an amplitude of $U_0 = 2$ kV and a frequency of $f = 13.7$ kHz, hence the period duration is equal to $T = 73$ µs. The model calculations are performed for a DBD in argon at the pressure of $p = 500$ mbar and constant gas temperature of $T_g = 300$ K. The computational domain is divided into the plasma region with 1500 mesh elements and the dielectric part with 50 elements. The reflection and secondary electron emission coefficients and corresponding energy of secondary electrons are taken as in [7]. The COMSOL model generated by MCPlas takes into account electrons plus 22 heavy particle species participating in 409 reaction kinetic processes. A list of the considered argon species with the corresponding energy levels is given in Table 1.

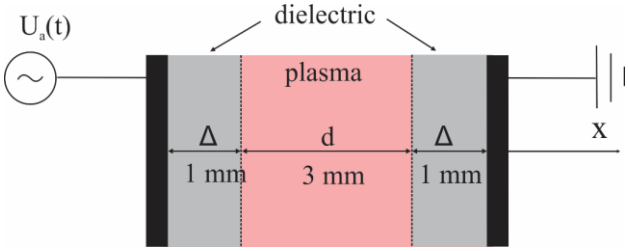

Figure 2. Schematic description of the spatially 1D DBD geometry used in test case 1.

Table 1. List of heavy particle species considered for the 1D modelling of a diffuse DBD in argon at 500 mbar (test case 1).

Species	Energy level [eV]
$Ar[1p_0]$	0
$Ar[1s_5]$	11.55
$Ar[1s_4]$	11.62
$Ar[1s_3]$	11.72
$Ar[1s_2]$	11.82
$Ar[2p_{10}]$	12.91
$Ar[2p_9]$	13.08
$Ar[2p_8]$	13.09
$Ar[2p_7]$	13.15
$Ar[2p_6]$	13.17
$Ar[2p_5]$	13.27
$Ar[2p_4]$	13.28
$Ar[2p_3]$	13.30
$Ar[2p_2]$	13.33
$Ar[2p_1]$	13.40
Ar*[hl]	13.84
Ar^+	15.76
$Ar_2[^3\sum_u^+, v = 0]$	9.76
$Ar_2[^1\sum_u^+, v = 0]$	9.84
$Ar_2[^3\sum_u^+, v >> 0]$	11.37
$Ar_2[^1\sum_u^+, v >> 0]$	11.45
Ar_2^+	14.50

The calculated discharge current I and gap voltage U_{gap} for the stable periodic state of the discharge reached after ten periods are shown in the Figure 3. Characteristic current peaks corresponding to the breakdown events can be noticed from the results. Also the temporal evolution of the gap voltage is in correlation with the calculated current showing the fast decrease at the moment of breakdown, which is caused by the charging of the dielectrics. Since the discharge current is mainly determined by the motion of electrons their maximum number densities are reached at the moment of the highest current. This is more obvious from the spatiotemporal evolution of the electron number density n_e presented in Figure 4. It can be seen that the highest number density of electrons appears at the instant of breakdown in front of the momentary cathode.

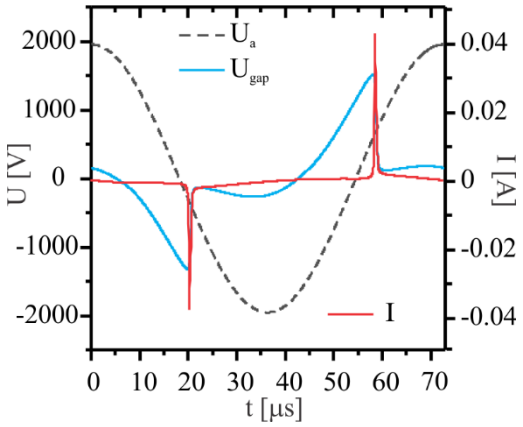

Figure 3. Temporal evolution of the discharge current and gap voltage obtained by the model for $p = 500$ mbar, $U_0 = 2$ kV and $f = 13.7$ kHz together with the voltage applied at the powered electrode.

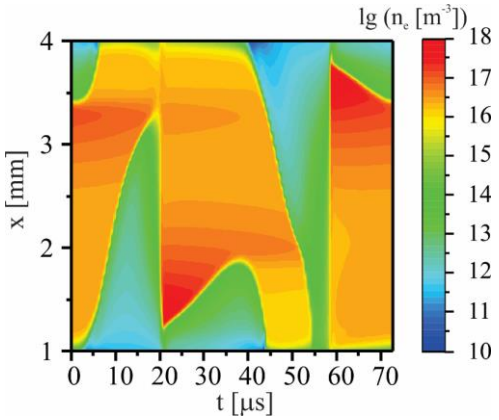

Figure 4. Spatiotemporal behaviour of the electron number density during one period for the conditions detailed in the caption of Figure 3.

Figure 5 shows the spatial distribution of the number densities of molecular (Ar_2^+) and atomic (Ar^+) ions and electrons as well as the magnitude of the electric field at the moment of maximum current in the negative half-period (t = 21.4 µs). Obviously, molecular argon ions are the dominant ionic species for these conditions. In addition, it is important to note that in front of the momentary cathode ($x = 1$ mm), the number densities of ions are higher than the number density of electrons. This leads to the formation of the cathode sheath with high electric field. All presented results for this test case are in accordance with results obtained by model calculations of the same type of DBD reported in the literature [7, 9].

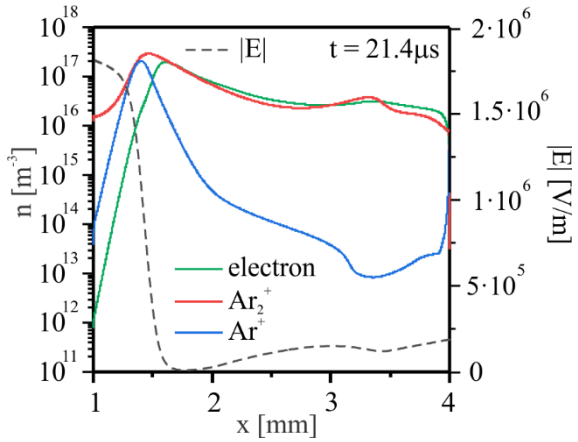

Figure 5. Number densities of electrons, argon atom ion Ar^+ and molecular ion Ar_2^+ in the moment of maximum current (t = 21.4 µs) for the conditions detailed in the caption of Figure 3.

Case 2: Modelling of a single-filament DBD in argon at atmospheric pressure

The second case study deals with 2D model calculations of a single-filament DBD in atmospheric-pressure argon. The asymmetric configuration shown in Figure 6 consists of two hemi-spherical electrodes with radius r = 2 mm and gap width d = 1.5 mm, in accordance with the setup investigated in [7, 10]. The grounded electrode is covered with a dielectric (alumina, ε_r = 9, thickness Δ = 0.5 mm), and the metallic electrode is powered by sinusoidal voltage. The voltage amplitude is set to be U_0 = 3 kV, and the frequency is f = 60 kHz.

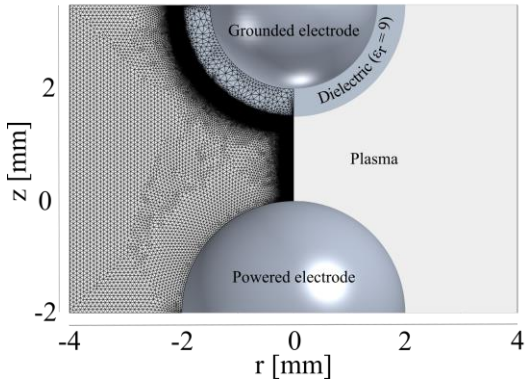

Figure 6. Schematic diagram of the asymmetric DBD configuration and used mesh.

For the axisymmetric 2D modelling of the filamentary DBD at these conditions, a reduced argon reaction kinetics considering electrons and five argon species is employed. Table 2 lists the argon species and their energy levels.

Table 2. List of heavy particle species considered for the 2D modelling of a single-filament DBD at atmospheric pressure (test case 2).

Species	Energy level [eV]
Ar[1p0]	0
Ar*	11.55
Ar^+	15.76
Ar_2*	11.27
Ar_2^+	14.50

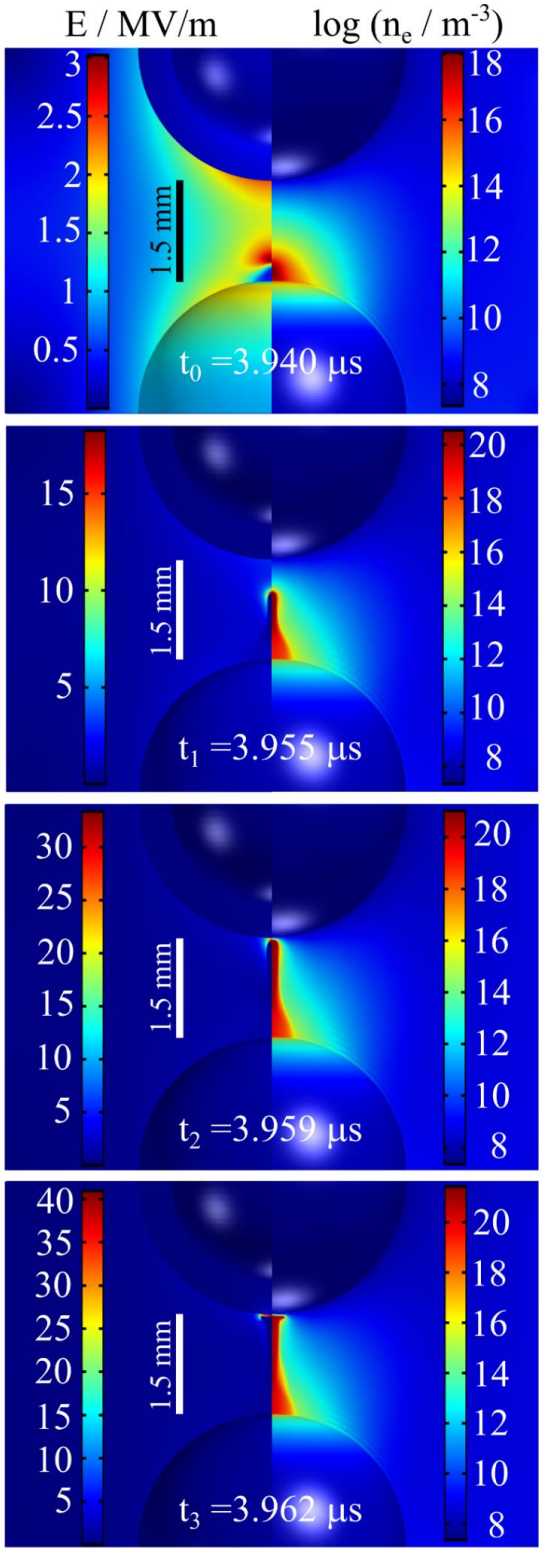

Figure 7. Spatiotemporal development of the streamer between the electrodes illustrated by the evolution of the electric field magnitude (left-hand-side panel) and electron number density (right-hand-side panel).

The focus of the analysis is on the streamer development in the gap during the first half-period. In this case, there are no volume and surface charges present in the gap or at the dielectric when the voltage is applied. In contrast to the first example, a 2D model is required to correctly describe the discharge because DBDs in argon at atmospheric pressure are

typically not diffuse but filamentary. Here, curved electrodes are used to fix one filament at the position with shortest electrode distance. Since the discharge is considered to be axisymmetric it is possible to solve the problem in cylindrical coordinates. The same surface coefficients and parameters as for the analysis of the diffuse DBD in test case 1 are used here as well. In order to reduce the calculation time, manual re-meshing of the domain is done. For the pre-phase covering the process of volume charge accumulation, a mesh consisting of approximately 60 000 elements is used, while for the streamer phase about 500 000 elements are required to resolve the steep gradients occurring at the streamer head. As shown in Figure 6 the mesh is refined near the symmetry axis and the dielectric surface with maximum element size of 4 μm near the axis and a mesh size varying between 0.1 and 1.3 μm near the plasma boundaries. In other parts of the domain, the mesh is much coarser with an element size in the order of 0.1 mm.

In order to illustrate the streamer development, the electron number density and magnitude of the electric field at characteristic times (t_0 - t_3) are presented in Figure 7. With increase of the applied voltage, Townsend's phase (pre-phase) commences, during which accumulation of space charges near the instantaneous anode occurs. When a critical density of charged particles is reached (approx. 10^{18} m^{-3}), the streamer phase is initiated (t_0 in Figure 7) and the positive streamer starts propagating in the gap (t_1 in Figure 7).

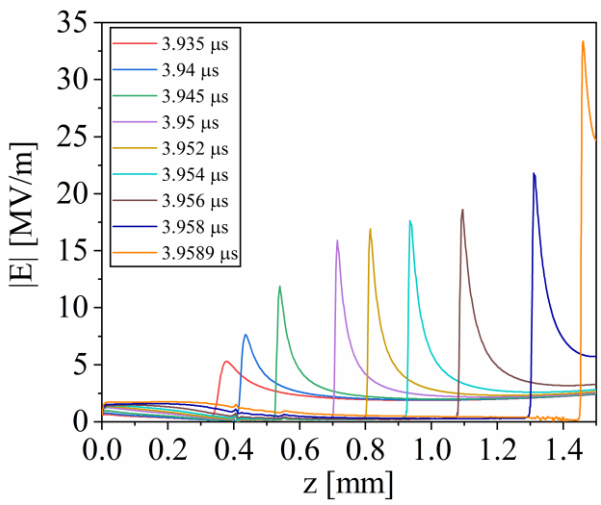

Figure 8. Magnitude of the electric field on the symmetry axis during streamer propagation. From the position of the maximum, the streamer velocity is determined.

Figure 8 shows the spatial variation of the magnitude of the electric field on the symmetry axis for different points in time. The maximum position of the electric field can be used to determine the streamer velocity v, which is represented in Figure 9. It can be observed that as the streamer propagates in the gap, its velocity increases. In the vicinity of the cathode (t_2 in Figure 7), the maximum streamer velocity of 0.17 mm/ns is reached (Figure 9). After reaching the cathode, the streamer starts propagating across the dielectric surface (t_3 in Figure 7). The surface streamer continues propagating along the dielectric surface until a sufficient amount of surface charges is accumulated on the dielectric, leading to the reduction of the electric field and charge carrier production in this region.

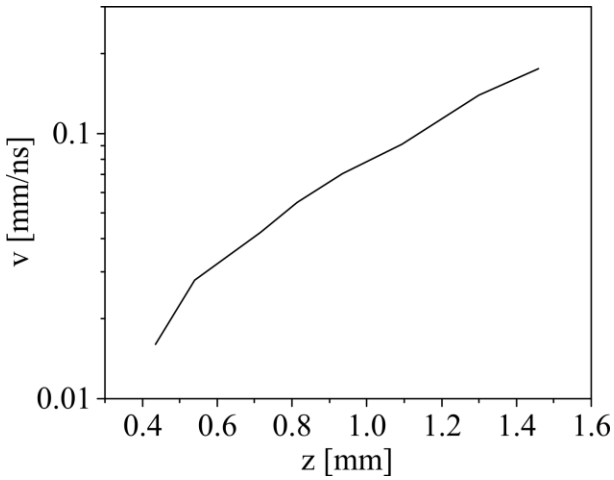

Figure 9. Development of the streamer velocity during streamer propagation. The maximum velocity is observed in vicinity of the cathode.

Conclusions

Fluid modelling is a powerful tool for the description of the physical and chemical processes occurring during plasma production in DBDs. However, the management of the equations and source term generation, as well as the definition of all required transport and rate coefficients can be a tedious and error-prone process when lots of particle species need to be taken into account. In order to overcome this by an automation of the model generation process, the MCPlas toolbox is developed using functionalities provided by the COMSOL module LiveLink™ for MATLAB®. The use of this code is illustrated by two case studies dealing with the analysis of a diffuse and a filamentary DBD in argon, respectively. It is shown that MCPlas allows one to easily generate COMSOL models for non-thermal plasmas even if many species and reaction kinetic processes need to be taken into account. The presented results confirm that COMSOL-based fluid modelling is a powerful tool for the computational analysis of non-thermal plasmas generated by DBDs for technological applications.

References

[1] A. Fridman, A. Chirokov, and A. Gutsol, TOPICAL REVIEW: Non-thermal atmospheric pressure discharges, *J. Phys. D: Appl. Phys.*, **38**, R1–R24 (2005)

[2] U. Kogelschatz, B. Eliasson, and W. Egli, Dielectric-Barrier Discharges. Principle and Applications, *J. Phys. France IV*, **7**, C4–66 (1997)

[3] R. Brandenburg, Dielectric barrier discharges: progress on plasma sources and on the understanding of regimes and single filaments, *Plasma Sources Sci. Technol.*, **26**, 053001 (2017)

[4] D. Braun, V. Gibalov, and G. Pietsch, Two-dimensional modelling of the dielectric barrier discharge in air, *Plasma Sources Sci. Technol.*, **1**, 166–174 (1992)

[5] G. Steinle, D. Neundorf, W. Hiller and M. Pietralla, Two-dimensional simulation of filaments in barrier discharges, *J. Phys. D: Appl. Phys.*, **32**, 1350–1356 (1999)

[6] L. Papageorghiou, E. Panousis, J. F. Loiseau, N. Spyrou, and B. Held, Two-dimensional modelling of a nitrogen dielectric barrier discharge (DBD) at atmospheric pressure: filament dynamics with the dielectric barrier on the cathode, *J. Phys. D: App. Phys.*, **42**, 105201 (2009)

[7] M. M. Becker, T. Hoder, R. Brandenburg, and D. Loffhagen, Analysis of microdischarges in asymmetric dielectric barrier discharges in argon, *J. Phys. D: Appl. Phys.*, **46**, 355203 (2013)

[8] G. J. M. Hagelaar, F. J. de Hoog, and G. M. W. Kroesen, Boundary conditions in fluid models of gas discharges, *Phys. Rev. E*, **62**, 1452–1454 (2000)

[9] F. Massines, A. Rabehi, P. Decomps, R. B. Gadri, P. Ségur, and C. Mayoux, Experimental and theoretical study of a glow discharge at atmospheric pressure controlled by dielectric barrier, *J. Appl. Phys.*, **83**, 2950 (1998)

[10] T. Hoder, D. Loffhagen, C. Wilke, H. Grosch, J. Schäfer, K.-D. Weltmann, and R. Brandenburg Striated microdischarges in an asymmetric barrier discharge in argon at atmospheric pressure, *Phys. Rev E*, **84**, 046404 (2011)

Acknowledgements

This work is funded by the Deutsche Forschungsgemeinschaft (DFG, German Research Foundation) - project numbers 368502453 and 407462159.